FIRE PROPERTIES WITH LONGITUDINAL VENTILATION IN A TUNNEL

Y. Oka[a], H. Kurioka[b], H. Satoh[b], and O. Sugawa[c]

a. Department of Safety Engineering, Yokohama National University

b. Kajima Technical Research Institute

c. Center for Fire Science and Technology, Science University of Tokyo

JAPAN

ABSTRACT

Experiments were conducted to characterise fire properties with longitudinal ventilation in a tunnel. Much of the focus was on flame shape, trajectory of hot current and effects of aspect ratio of a tunnel cross-section on these variables. Three types of model tunnel, having rectangular and horseshoe cross-sections, were employed. The aspect ratios, defined as height divided by width, ranged from 1/1 to 1/3. The flame tilt-angle from the vertical was obtained using the isotherm curves constructed with measured temperatures. An empirical model is proposed for the flame tilt-angle based on the balance of mass fluxes given by the upward hot current and longitudinal ventilation velocity. Empirical models for maximum temperature of smoke layer under the ceiling and its position are also presented.

Keywords: Tunnel fire, longitudinal ventilation, aspect ratio, flame tilt.

INTRODUCTION

The choice of smoke exhaust equipment often depends on tunnel length and traffic volume. A common mechanical system is the longitudinal ventilation flow system for one-way traffic road tunnels. This forced ventilation significantly affects flame properties and flow behaviour of combustion products.

By increasing demands for longer and larger cross sectional-area tunnels to cut transport time (high-speed running) and strengthen the capacity of transport, situations that cannot be handled with conventional fire prevention measures arise. It is therefore necessary to establish new measures considering the cross-sectional shape of tunnels, fire source shape and location etc. to prevent tunnel

fires or to reduce their spread. In other words, fire-prevention engineers must consider not only the damage to the structures and objects around the fire source but also the influence on evacuation planning and rescue operations.

Most papers on tunnel fires have paid attention to smoke control, such as critical velocity, to prevent upstream movement of combustion products in forced ventilation[1-6] and smoke movement in natural ventilation[7-9]. Few papers have reported on addressing the behaviour of flames affected by forced longitudinal ventilation and the fire phenomena in the near field of the fire source[10,11].

The objective of the current work was to understand experimentally fire properties in the near field of a fire source since they become key parameters of smoke propagation. Attempts have also been made to develop empirical models to predict and describe not only the tilt angle of the flame but also the maximum temperature of the smoke layer and its location under the tunnel ceiling.

DEFINITION OF VARIABLES AND DERIVATION OF MODEL FORMULA

Definition of flame tilt angle in a tunnel

In an unconfined space, the flame tilt angle affected by cross-winds is often defined as the angle formed by the straight line between the centre of the burner surface and the flame tip. From observations of flame development in a tunnel fire, there appear to be two largely different types of flame that should be considered when determining the flame tilt angle, one that collides with the tunnel ceiling and the other that does not. While the given definition of flame tilt angle in an unconfined space would be applicable for flames not touching the ceiling, it is difficult to determine a well-defined position of the flame axis touching the ceiling by the angle formed by the straight line.

Two kinds of angle were chosen, θ_1 and θ_2, to define the flame tilt as shown in Figure 1. Both these tilt-angles were measured from the vertical. In this study the flaming region is defined by temperature and not by a visual record. Hence, the accuracy of the tilt angle depends strongly on the temperature of the isotherm used to delineate the flame. The region over $\Delta T = 250$ K is employed to define the flaming region.

Definition of other variables

The upward velocity close to the fire source has relatively weak buoyancy compared to the potential of longitudinal ventilation and the flame is pushed downstream, showing a spread at the base of the flame. The upward velocity, however, gradually increases as buoyancy increases with height and flames tend to rise vertically. The locus of trajectory of flame and/or hot current was then assumed as follows. The axis of flame and/or hot current is pushed downstream at distance X_1 from the centre of the burner and rises at the angle θ_1 and collides with the tunnel ceiling. Flame and/or hot current, which collided with the ceiling, propagates in upstream and downstream directions from the collision point, but only the propagation downstream is considered in this paper. At longer travelling distances of hot current, the buoyancy becomes weaker, and the head of hot current then falls down and mixes with the local air which is colder. However, the hot current, which touched the ceiling, is considered to remain sufficiently hot in the near field of the fire source. This is because the heat supplied to the smoke layer from the fire source is much lager than that carried out by convection from the smoke layer to the tunnel boundary. It is therefore considered that the hot current does not separate from the ceiling in this region. This modeled trajectory is shown in Figure 2 by a solid line.

The straight line from the centre of the burner surface to the position that the flame and/or hot current collided with the tunnel ceiling is defined as L. The maximum temperature of the smoke layer under the tunnel ceiling is also defined as ΔT_{max} and it is assumed that this position coincides with the position that the flame and/or hot current collided with the tunnel ceiling. Moreover, the length from this point downstream is defined as X_3. These variables are shown in Figure 2.

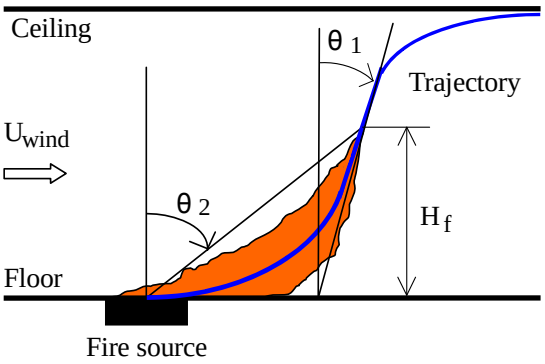

Figure 1(a): Definition of the tilt angle and length of flame. Flames without touching to tunnel ceiling.

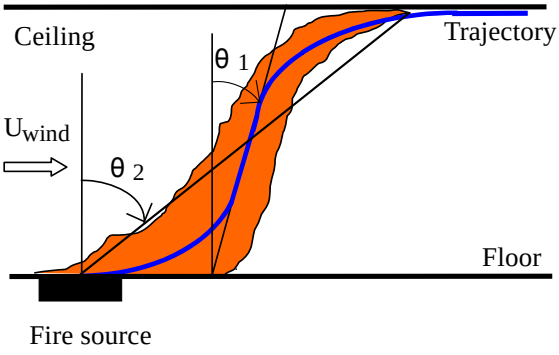

Figure 1(b): Definition of the tilt angle and length of flame. Flames with touching to tunnel ceiling.

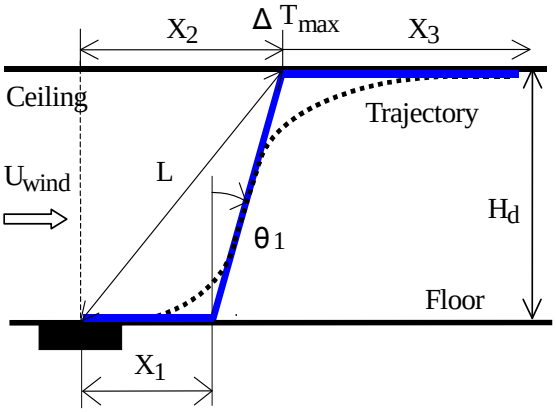

Figure 2: Definition of other variables. Dotted and solid lines mean real and modeled trajectory, respectively.

Derivation of model formula

An expression can be obtained for flame inclination in a tunnel by modifying equations applied to unconfined spaces, restricted to the case of the flame not touching to the tunnel ceiling[11]. Therefore, it is possible to develop an alternative model based on the following assumptions.

(a) Shape of the fire source is a square or a circle.

(b) Cross-sectional shape of the tunnel is a rectangle.

(c) Opening diameter, $\sqrt{A_S}$, for the mass flux flowing into the tunnel through the opening and diameter of fire source, $\sqrt{A_f}$, for that carried by the inclined fire plume are respectively adopted as a reference length.

(d) Moderate forced ventilation is operating, namely not becoming one layer well-mixed but upper hot and lower cold layers are formed.

(e) The centerline properties proposed by McCaffrey[12] are succeeded in the presence of longitudinal forced ventilation.

It is assumed that the mass flux created by the longitudinal forced ventilation velocity passing through the tunnel balances that of the upward hot current due to the buoyancy at the curved surface including flame axis. It can then be shown that[10]:

$$\rho_o \cdot U_{wind} \cdot H_d \cdot A_s^{1/2} \propto \rho_f \cdot W \cdot L \cdot A_f^{1/2} \quad (1)$$

The formula proposed by McCaffrey is substituted into Equation 1, and normalised by the vertical length from the burner surface to ceiling, H_d. The final equation for flame tilt angle is given in Equation 2:

$$\cos\theta_2 \propto \left(\frac{A_f}{A_s}\right)^{1/2} \cdot Q^{*\frac{1-2\eta}{5}} \cdot Fr^{-\frac{1}{2}} \quad (2)$$

where η is the relative positional relationship between flame and tunnel ceiling. Three regions were employed according to the maximum temperature of the smoke layer under the tunnel ceiling and employed $\Delta T = 250$ and 550 K as boundary temperatures. It was also assumed that it attains a value of $\eta =$ 1/2, 0, and -1/3 in each region[10].

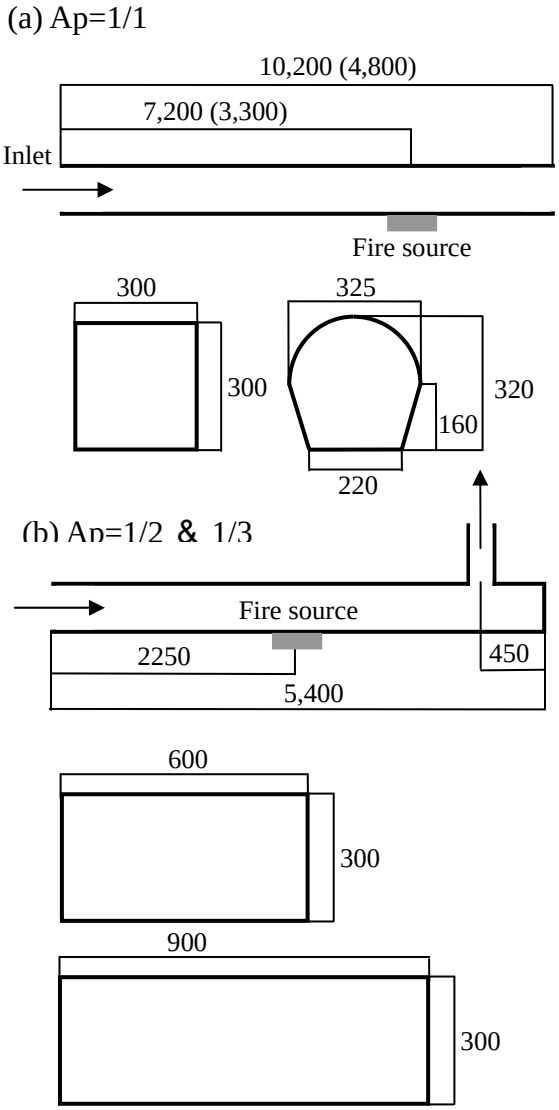

Figure 3: Schematic diagram of the model tunnels employed in this study. (a) Ap=1/1 tunnel, (b) Ap=1/2 & 1/3 model tunnels. unit: mm.

The expression for the distance from the centre of the burner surface to the position of the maximum temperature of the smoke layer under the tunnel ceiling can be obtained by employing the following techniques.

$$\frac{L}{H_d} \propto \left(\frac{As}{Af}\right)^{1/2} \cdot Fr^{\frac{1}{2}} \cdot Q^{*\frac{2\eta-1}{5}} \quad (3)$$

where, H_d was adopted as a reference length for calculating *Fr* and *Q**.

EXPERIMENTAL PROCEDURE

Figure 3 shows a schematic diagram of the experimental apparatus. Three model tunnels were employed with different aspect ratios (*Ap*), defined as height divided by width. The major part of each model tunnel was made of steel plate with a thickness of 3 mm, with the ceiling lined with 10 mm thick fireproof blanket to a distance of 45 cm in both directions from the fire source. In the case of *Ap*=1/1, two model tunnels were employed, shown in Figure 3 (a). One had a 0.3 m x 0.3 m square cross section, the other had a horseshoe shape, 0.32 m from the floor to the apex of the roof with a width of 0.22 m at floor level (maximum width was 0.325 m). These model tunnels had the same cross-sectional area of 0.09 m^2. Two lengths were used for each tunnel, 4.8 m and 10.2 m. In the case of *Ap*=1/2 and 1/3, they had 0.3 m x 0.6 m and 0.3 m x 0.9 m rectangular cross sections and each model was 5.4 m in length.

A square porous burner, 0.1 m x 0.1 m, was used as a model fire source in all experiments and set with its top surface adjusted the same level as the tunnel floor. Liquefied propane gas was employed as fuel. Experimental conditions for heat release rates and nominal longitudinal ventilation velocities are listed in Table 1.

A longitudinal ventilation flow was supplied from the rectangular duct, whose dimensions were 0.3 m x 0.3 m, connected to the fan via a honeycomb filter in the model tunnel of *Ap*=1/1. The downstream opening was fully open so as not to restrict air flow. There was also smoke extraction fan installed at the exhaust side in the model tunnel of *Ap*=1/2 and 1/3. The upstream opening was fully open but the downstream opening at the end of tunnel was closed.

The ventilation velocities listed in Table 1 were predefined values. A representative mean longitudinal ventilation velocity was employed, by dividing the measured total volumetric flow by the effective cross-sectional area of each model tunnel for the analysis.

Table 1: Experimental conditions for heat release rates and nominal longitudinal ventilation velocities.

Ap	**Heat release rate (kW)**	**Nominal longitudinal ventilation velocity (m/sec)**	**Ventilation method**
1/1	1.5, 3.0, 6.0, 8.0, 12.0, 14.0, 21.0	0.1, 0.3, 0.5, 1.0	blow a fresh air into the tunnel
1/2	1.5, 3.0, 6.0, 12.0	0.2, 0.3, 0.4, 0.6, 1.0	suction smoke from the tunnel
1/3	1.5, 3.0, 6.0, 12.0	0.2, 0.4, 0.5, 0.7	suction smoke from the tunnel

The temperature field generated by the tilted flame was measured using K-type thermocouples with a diameter of 0.65 mm. Thermocouples were set at 10, 115, 165, 215, 265 and 290 mm heights and in every 50 mm interval to cover a downward region of 0.65 m(W) x 0.29 m(H) along the longitudinal axis of the tunnel with the datum set at the centre of the burner. Temperature of the smoke layer was

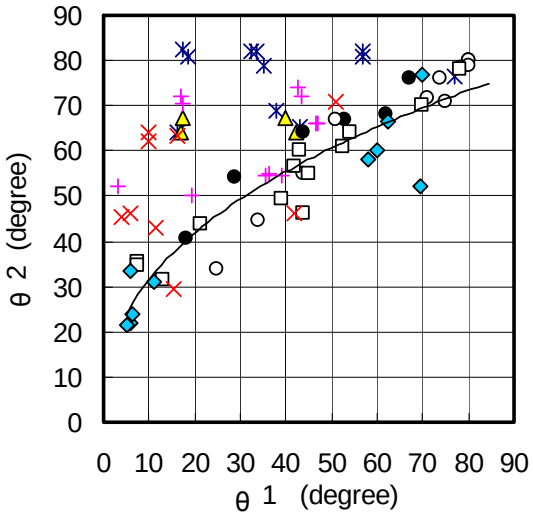

Figure 4: Relation between θ_1 and θ_2.

also measured at 10 mm below the tunnel ceiling. Details of other temperature measurement grids were found in the literature[14]. Isotherm curves were constructed using these temperatures to obtain the tilt angle of flame and/or hot current axis and various lengths. Depending on the heat release rate and the magnitude of the longitudinal ventilation velocity, the flame tip sometimes extended beyond the net of thermocouples to make it impossible to delineate the flaming region. Values for temperature were taken as an average over the last 3 min of a 10 min test, this duration being assumed to be at a quasi steady state for both heat release rate and longitudinal ventilation velocity.

RESULTS AND DISCUSSIONS

Relation between θ_1 and θ_2

Figure 4 shows the relationship between θ_1 and θ_2. In the case of flames not touching the tunnel ceiling, the angle defined by θ_2 was slightly larger than that defined by θ_1. The correlation between θ_1 and θ_2 can be recognised, regardless of the aspect ratio of the model tunnel. The correlation for θ_1 and θ_2 is given as follows:

$$\theta_2 = \alpha(\theta_1)^{\beta} \tag{4}$$

$\alpha = 12.4$, $\beta = 0.4$, correlation coefficient =0.8901

It is difficult, however, to find a clear correlation between θ_1 and θ_2 in the case of the flame touching the tunnel ceiling. After flames collide with the tunnel ceiling, they extend their length along the ceiling and then the angle defined by θ_2 is much larger than that defined by θ_1. Therefore, it was not appropriate to represent the position of the flame and/or hot current axis by θ_2. For this reason, θ_1 becomes a more useful parameter for tilt angle regardless of whether the flames touch the tunnel ceiling or not.

Characteristics of flame tilt angle (θ_l)

It was assumed that the relationship represented in Equation 2 was applicable to θ_l. Figure 5a shows the relationship between the measured tilt angles, θ_l, and the combination function of reference length, *Fr* and *Q**. Although an orderly relationship exists between the tilt angle and the combination function over whole regions, this figure indicates that Equation 2 does not become the universal expression. The cause seems to arise from not considering the effect of the aspect ratio of the tunnel cross-section. A new variable for representing the effect of aspect ratio was therefore introduced. This variable, $H^{3/2}/b^{1/2}$, was deduced from the results showing that temperature decreased along the centreline of a fire plume from the fire source surface to the tunnel ceiling in the absence of forced ventilation. The result of rearranging with the function which substituted $H^{3/2}/b^{1/2}$ instead of $\sqrt{A_S}$ is shown in Figure 5b. Although the dispersion was seen, the improvement was recognised in comparison with the result shown in Figure 5a. The final formula for tilt angle, considering the aspect ratio is given in Equation 5.

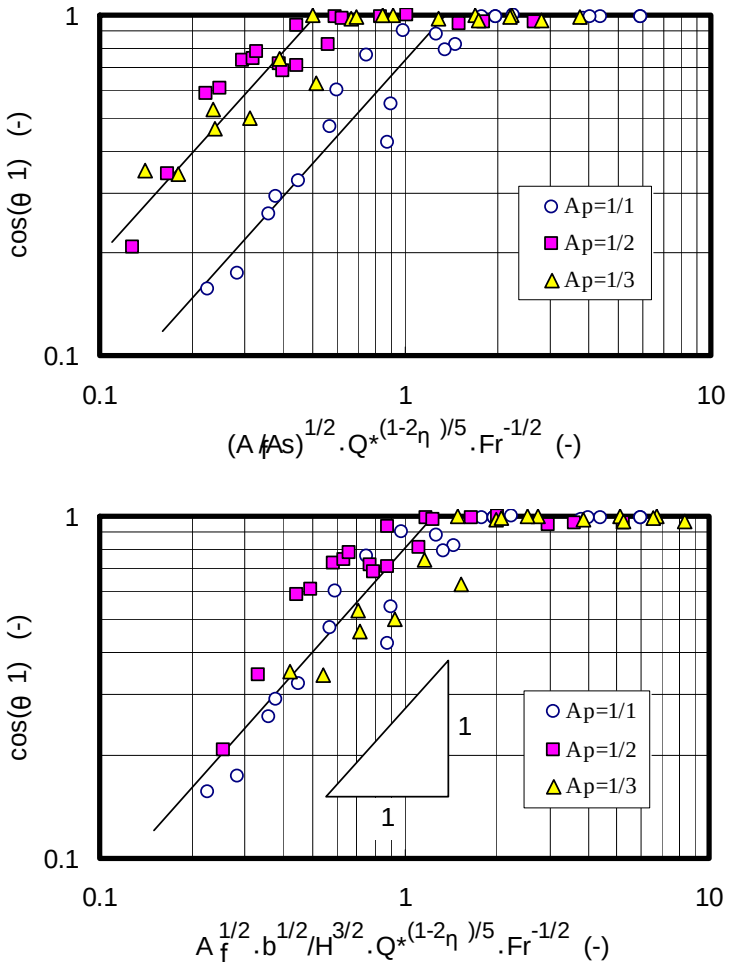

Figure 5: Variation of tilt angle against the function of *Q** and *Fr*.
(a) Data are plotted according to the empirical formula which is deduced using the data of Ap=1/1, as shown in the literature[10].

(b) Data are plotted considering the fire source area and the aspect ratio of tunnel cross section. Solid line means equation (5).

$$\cos\theta_1 = 0.80\left[A_f^{1/2}\cdot\frac{b^{1/2}}{H^{3/2}}\cdot Q^{*\frac{1-2\eta}{5}}\cdot Fr^{-\frac{1}{2}}\right] \qquad 0.15 \le A_f^{1/2}\cdot\frac{b^{1/2}}{H^{3/2}}\cdot Q^{*\frac{1-2\eta}{5}}\cdot Fr^{-\frac{1}{2}} < 1.25$$

$$\cos\theta_1 = 1 \qquad 1.25 \le A_f^{1/2}\cdot\frac{b^{1/2}}{H^{3/2}}\cdot Q^{*\frac{1-2\eta}{5}}\cdot Fr^{-\frac{1}{2}} \qquad (5)$$

The value of η is decided in every region, which is judged based on the value of ΔT_{max}. Equation 5 holds only when the surface of the fire source is positioned at the level of the tunnel floor. It does not yet include the effects of fire source, shape or position.

Maximum temperature of smoke layer under tunnel ceiling

An attempt was made to develop an empirical formula for directly estimating the maximum temperature as a function of Q^* and Fr. As shown in Figure 6, the data can be matched closely by the following expression, Equation 6, irrespective of the value of the aspect ratio.

$$\frac{\Delta T_{\max}}{T_a} = \alpha\left(\frac{Q^{*2/3}}{Fr^{1/3}}\right)^{\beta} \qquad (6)$$

$$\begin{cases} Q^{*2/3}/Fr^{1/3} < 1.35\ ,\ \alpha = 1.77\ ,\ \beta = 6/5 \\ 1.35 \le Q^{*2/3}/Fr^{1/3}\ ,\ \alpha = 2.54\ ,\ \beta = 0 \end{cases}$$

In the range of the present experimental results, the maximum excess temperature of the smoke layer was about 800 K. The temperature at the fire accident in the Mont Blanc Tunnel was reported to have reached over 1000 K. It is considered that there is an end-point for the temperature rise as an upper limit. Therefore, $\Delta T_{max}/T_a$ becomes independent of the combination function of Fr and Q^*. In this study, this upper limit for excess temperature was set at 770 K.

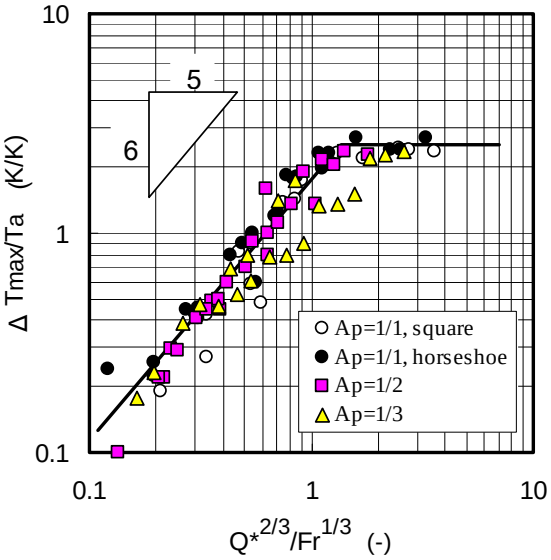

Figure 6: Variation of maximum temperature of smoke layer under the tunnel ceiling against the function of Q^* and Fr.

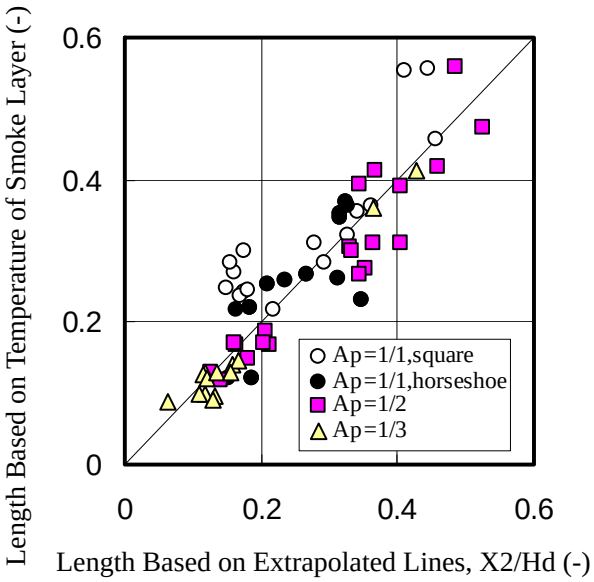

Figure 7: Relation between length based on temperature distribution of smoke layer and that on position where fire plume axis collides with the tunnel ceiling, latter data were obtained from isotherm curves.

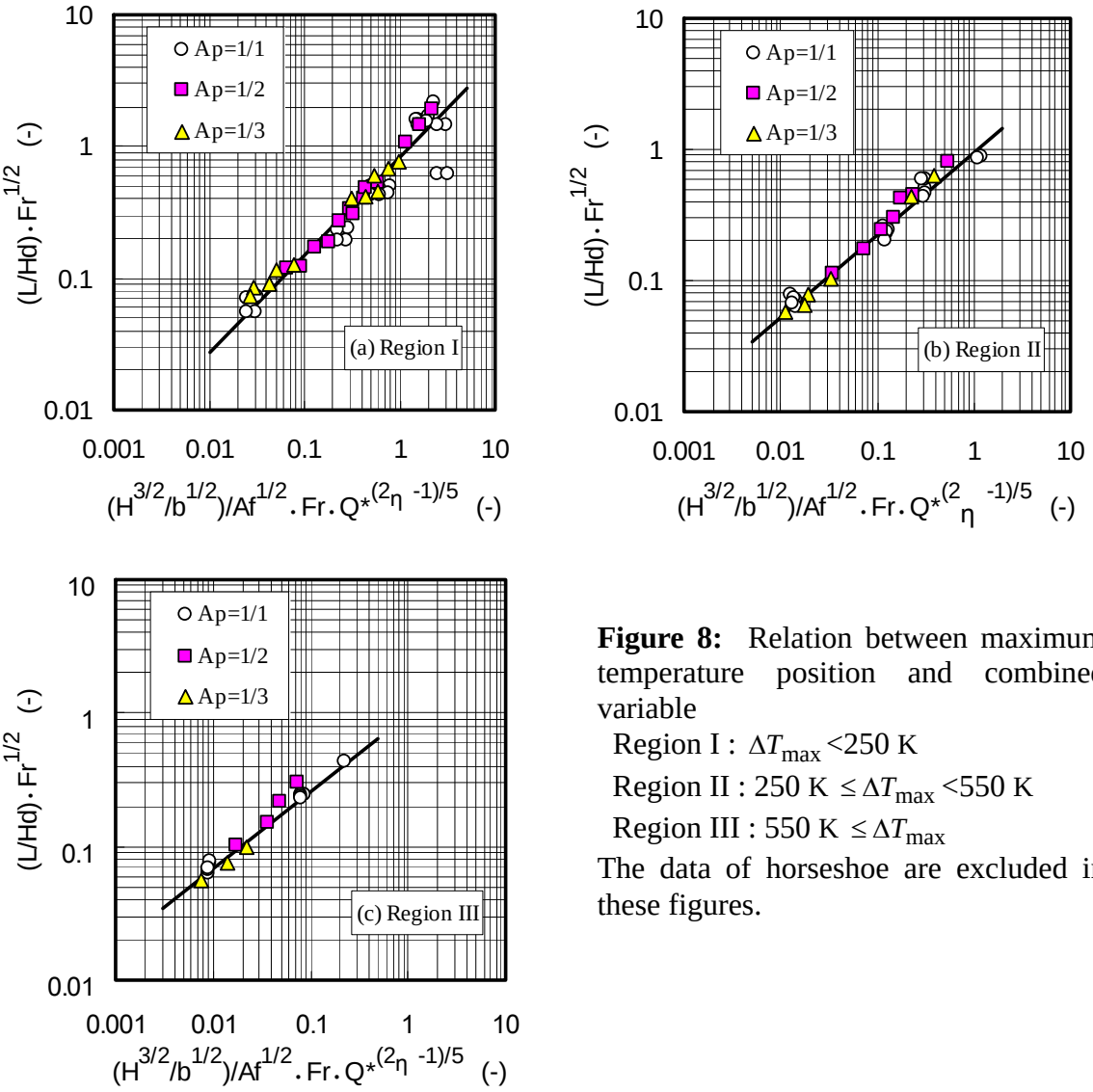

Figure 8: Relation between maximum temperature position and combined variable

Region I : ΔT_{max} <250 K

Region II : 250 K $\leq \Delta T_{max}$ <550 K

Region III : 550 K $\leq \Delta T_{max}$

The data of horseshoe are excluded in these figures.

Maximum temperature position

Figure 7 shows the relationship between the positions of maximum temperature that appeared under the ceiling. These data were obtained based on temperature distributions of the smoke layer, and the extrapolated lines along the flame/plume axis colliding with the tunnel ceiling. These positions were read from the isotherm curves. The maximum temperature of the smoke layer was considered to exist in the vicinity of the position where the flame or hot current axis collided with the tunnel ceiling.

These maximum temperature positions were plotted against the function described by Equation 3 after substituting $H^{3/2}/b^{1/2}$ instead of $\sqrt{A_S}$ as shown in Figure 8. The values of empirical coefficients and exponents were decided in every region as listed below. The final expression for L is given in Equation 7:

$$\frac{L}{H_d} \cdot Fr^{1/2} = \alpha \left[\left(H^{3/2} / b^{1/2} \right) \Big/ A_f^{1/2} \cdot Fr \cdot Q*^{(2\eta - 1)/5} \right]^{\beta} \qquad (7)$$

Table 2: Summary of coefficients and exponents employed in equation (7) in each region.

	η	α	β	ΔT_{max}
Region I	-1/3	0.836	0.745	<250 K
Region II	0	0.949	0.626	250~550 K
Region III	1/2	0.960	0.572	≧ 550 K

The position of inclined flame axis is defined as follows:

Firstly, the maximum temperature under the ceiling is calculated using Equation 6. Secondly, the length, L is calculated using Equation 7 with the value of η which is defined in each region. The region is determined by ΔT_{max}. Finally, the position of the inclined flame axis is defined by describing the straight line from the maximum temperature position with the value of θ_1 from the vertical. The angle θ_1 is calculated using Equation 5.

Prediction of the flame tip position in the case of the flame not touching tunnel ceiling

The flame in tunnels is affected by of the spatial structure elements such as the ceiling and sidewalls. The difference in the aspect ratio of the tunnel cross-section is represented as a change of the distance from the centre of fire source to the sidewall. It was assumed that the change of distance to the sidewall affects the condition for restricting the flame behaviour. Then the value of power of Fr_{-D} was varied.

In the case of flames not touching the tunnel ceiling, it is assumed that the effect of tunnel ceiling for flame behaviour was weaker than that of sidewall and floor. In the case of Ap=1/1, the effect of the sidewall was added as the condition for restricting flame behaviour in comparison with the condition in unconfined space. By reducing one degree of freedom of the longitudinal ventilation flow it was made to be n=1/3. In the case of Ap=1/2 and 1/3, with the tunnel cross-section enlarging in the perpendicular direction of the tunnel axis, the restricting effect of the sidewall to the flame behaviour would be decreased. Then it was set at n=2/3. This value, n=2/3, is equal to the value for the cross-winds on the flame inclination for the situation when the burner is positioned at the same level of artificial floor in an unconfined space[13].

The result for the apparent flame height against the combination function of Fr_{-D} and Q^*_{-D} based on the

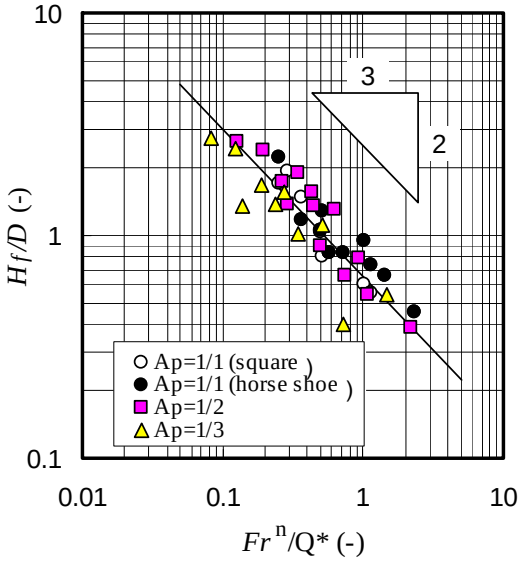

Figure 9: Variation of the apparent flame height against combined variables, Q^*_{-D} and Fr_{-D} without flames touching the tunnel ceiling.

earlier ideas is shown in Figure 9. It is considered that the value of power of Fr_{-D} continuously changes from n=1/3 to 2/3 depending on the occupied area of the flame to the cross-sectional area of the tunnel. However, it was impossible to find the clear relationship in this study. Although there is some dispersion, the apparent flame height was arranged by considering the effect of the aspect ratio of the tunnel cross-section as given in Equation 8. The value of the intercept changes slightly depending on the aspect ratio when they were compared in detail. The value of the intercept was decided on the basis of the whole data set obtained in Tunnel A, B and C.

$$\frac{H_f}{D} = 0.65\left(\frac{Fr_{-D}^{n}}{Q_{-D}^{*}}\right)^{-2/3} \qquad 0.07 \le \frac{Fr_{-D}^{n}}{Q_{-D}^{*}} \le 3 \tag{8}$$

Ap=1/1 n=1/3, Ap=1/2, 1/3 n=2/3

The empirical formula expressed in Equation 8 is applicable only under the presence of ventilation, because the height of the flame becomes infinite under the absence of longitudinal ventilation.

The value of the power of the combination function of Fr_{-D} and Q^*_{-D} becomes –3/4 in unconfined space[13] and –2/3 in the tunnel. Considering that the data of the apparent flame height were read from the isotherm curves, the temperature decreasing tendency in the tunnel shows slower decreasing than that in unconfined space. It becomes experimentally clear that fire plume width in the tunnel under the absence of forced ventilation becomes 2 to 3 times wider than that in unconfined space regardless of the aspect ratio[10]. If assuming that the fire plume retains the wider shape under the presence of forced ventilation and suppresses the diffusion of heat to the tunnel wall, the temperature decreasing tendency to the downstream becomes slower.

Prediction of the flame tip position in the case of flame touching to tunnel ceiling

In order to estimate where the flame tip is located in the case of the flame touching the tunnel ceiling, the temperature decreasing property was investigated, because the temperature range over 250 K was defined as the flaming region. The temperature decreasing rate against travel distance to the downstream side from the point where the maximum temperature appeared was arranged for every aspect ratio. It was assumed that decreasing coefficients and intercepts obtained by the statistical processing could be represented by the function of the aspect ratio and they were given using linear functions. The final expression for temperature decrease of the smoke layer against travelling distance is given in Equation 9:

$$\frac{\Delta T}{\Delta T_{\max}} = \alpha\left(\frac{X_3}{H_d}\right)^{\beta} \qquad 0.2 \le X_3 / H_d \le 8 \tag{9}$$

$$\alpha = 0.40Ap + 0.31, \quad \beta = 0.51Ap - 0.72$$

CONCLUSIONS

Properties of flame and fire phenomena in the near field of fire source were studied using three types of model tunnel, which the aspect ratio of cross-section ranging from 1/1 to 1/3, under the presence of longitudinal forced ventilation.

It was not always appropriate to use the angle formed by simply linking the fire source and the flame tip to define the tilt angle of flame axis in a tunnel. Instead, the angle created by the intersection of the floor level and extrapolated flame axis is recommended, irrespective of whether the flame touches to the tunnel ceiling or not.

A new expression has been developed to predict the flame tilt angle regardless of whether flames touch the tunnel ceiling or not. This model was derived from the balance of mass fluxes of longitudinal forced ventilation velocity and hot air current, combined with centreline properties of a fire plume. The relational expressions, which estimated maximum temperatures of smoke layers under the tunnel ceiling and their position, were also proposed.

It is possible to represent the effect of the cross-section of a tunnel by employing $H^{3/2}/b^{1/2}$ instead of $\sqrt{A_S}$ as a representative length in tunnel.

A dimensionless equation for the apparent flame height of an inclined flame under the presence of forced ventilation in a tunnel has been developed based on the dimensionless heat release rate and Froude number. This equation is available only in the case of flames not touching the tunnel ceiling.

Temperature decreasing properties downstream, along the tunnel axis from the position where the maximum temperature appears, is represented considering the effect of the aspect ratio.

ACKNOWLEDGMENTS

The authors wish to express our sincere gratitude to Mr. Hideaki Kuwana and Mr. Yoshiaki Arai of Kajima Technical Research Institute, Mr. Norichka Kakae and Miss. Yuko Kunikane of Yokohama National University who kindly cooperated in conducting the experiments.

NOMENCLATURE

A_S	cross-sectional area of model tunnel (m^2)
A_f:	area of fire source (m^2)
A_p	aspect ratio of tunnel cross-section, defined as height divided by width (-)
B	tunnel width (m)
C_p	specific heat at constant pressure (kJ/kg.K)

D	representative length of fire source (m)
H	model tunnel height (m)
H_d	height from the surface of fire source to tunnel ceiling (m)
g	acceleration due to gravity (m/sec^2)
L	distance from the position that flame and/or hot current axis collided with the tunnel ceiling to the centre of fire source (m)
Q	heat release rate (kW)
T_a	ambient temperature (K)
ΔT	excess temperature (K)
ΔT_{max}	maximum excess temperature of smoke layer at downstream region (K)
U_{wind}	representative longitudinal ventilation velocity (m/s)
W	upward velocity due to the buoyancy in the dominant region (m/s)
X_1	horizontal length from the intersection created by the extrapolated plume axis to the centre of the burner surface (m)
X_2	horizontal length from the centreline of fire source to the position showing maximum temperature of smoke layer (m)
X_3	horizontal length from the position showing maximum temperature of smoke layer to the downstream (m)

Greek symbols

α , β : constants of experiment

η : coefficient determined in every region

θ_1: the angle created by the intersection of the floor level and extrapolated flame/plume axis.

θ_2: the angle formed by the straight line between the centre of the burner surface and the intersection of the flame axis and the front of the isotherm curve of ΔT =250 K

ρ_a : density of ventilation air (kg/m^3)

ρ_f : density of hot current in the dominant region (kg/m^3)

Dimensionless groups

$$Fr = U_{wind}^2 /(g \cdot H_d)$$

$$Q^* = Q/(\rho_a C_p T_a g^{1/2} H_d^{5/2})$$

$$Fr_{-D} = U_{wind}^2 /(g \cdot D)$$

$$Q^*_{-D} = Q/(\rho_a C_p T_a g^{1/2} D^{5/2})$$

REFERENCES

1 Bettis, R. J., Jagger, S. F. and Macmillam, A., "Interim Validation of Tunnel Fire consequence Models: Summary of Phase 1 Tests", HSL Report No. IR/L/FR/94/2, 1994.

2 Oka, Y. and Atkinson, G.T., "Control of Smoke Flow in Tunnel Fires", Fire Safety Journal, Vol.25, pp.305-322, 1995.

3 Grant, G.B., Jagger, S.F. and Lea, C.J., "Fires in tunnels", Phil. Trans. R. Soc. Lond. A, Vol.356, pp.2873-2906, 1998.

4 Wu, Y. and Bakar, M.Z.A., "Control of smoke flow in tunnel fires using longitudinal ventilation systems – a study of the critical velocity", Fire Safety Journal, Vol.35, pp.363-390, 2000.

5 Yamada, T., et al., "Experiment of Upward Smoke Propagation at Tunnel Fire", Report of Fire Fighting Research Institute, Vol. 83, 1997, in Japanese.

6 Lea, C. J. "Computational Fluid Dynamics Simulations of Fires in Longitudinally-Ventilated Tunnels", HSL Report No. IR/L/FR/94/10 , 1995.

7 Matushita, T. et. Al., "Mathematical model and Experiments of Axisymmetric Spread of Smoke Front under Ceiling", Part I, & Part II, Bulletin of Japanese Association for Fire Science and Engineering, Vol.48, No.1, pp.19-24, 1998, Vol.48, No.2, pp.1-8, 1998, in Japanese.

8 Handa, T et al. "Studies on the Motion and the Thermal Behaviors of Fire Products through Full Scall Corridor", Bulletin of Japanese Association for Fire Science and Engineering, Vol.28, No.2, pp.1-9, 1978, in Japanese.

9 Kitahara, R. and Umezu, M., "Study on the Hoy-Layer Behaviors in Tunnel Fires Part I Experimental Study of Ceiling Hot-Layer", Bulletin of Japanese Association for Fire Science and Engineering, Vol.34, No.1, pp.7-15, 1984, in Japanese.

10 Kurioka, H., Oka, Y., Satoh, H., Kuwana, H. and Sugawa, O., "Properties of Plume and Near Fire Source in Horizontally Long and Narrow Spaces", Journal of Constr. Engng, AIJ, No.546, pp.151-156, 2001, in Japanese.

11 Oka, Y., Kurioka, H., Satoh, H., and Sugawa, O., "Flame Properties with Longitudinal Ventilation in a Tunnel Fire -In case of flames without touching tunnel ceiling-", Bulletin of Japanese Association for Fire Science and Engineering, vol.51, No.2, pp.1-12, 2001, in Japanese.

12 McCaffrey, B.J., "Purely buoyant diffusion flames: some experimental results", NBSIR 79-1910, 1979.

13 Oka, Y., Kurioka, H., Satoh, H. and Sugawa,O., "Modelling of Unconfined Flame Tilt in Cross-Winds", Int. Assoc. of Fire Safety and Science, Proceedings of the 6th International Symposium on Fire, pp.1101-1112, 2000.

14 Kakae, N., "Experimental Study on Fire Phenomena in Underground", master's thesis of Yokohama National University, 2001, in Japanese.